SUBSURFACE DEFORMATION OF EXPERIMENTAL HYPERVELOCITY IMPACTS IN QUARZITE AND MARBLE TARGETS. R. Winkler[1], M. H. Poelchau[1], C. Michalski[2], T. Kenkmann[1], [1]Institute of Earth and Environmental Sciences – Geology, Albertstraße 23B, 70104 Freiburg, Germany rebecca.winkler@geologie.uni-freiburg.de, [2]Fraunhofer Ernst-Mach-Institute, Eckerstraße 4, 70104 Freiburg, Germany.

Introduction: During hypervelocity impact the crater subsurface experiences pervasive deformation. The formation of new pore space through dilation as well as the reduction of preexisting pore space through compaction has implications e.g., for the gravity anomaly signatures of impacts [1]. Fracture propagation and the localization behavior of damage depend on mechanical properties of the rock, i.e., dynamic strength behavior, which in turn must be constrained by the mechanical properties of the rock-forming minerals phases. Due to mineral cleavage, strength anisotropies, grain boundary cohesion, etc. different non-porous rock types can develop distinct deformation patterns under similar impact conditions. These patterns also correspond to the variation of the stress field that occurs during the propagation of the shock wave. Deformation features that commonly occur in non-porous rocks develop subsequently during an impact. Where pressures in the order of a several GPa above the Hugoniot Elastic Limit (HEL) are achieved, non-porous rocks fail under compression, due to pervasive shearing under differential stresses [2]. When pressures decrease to around the HEL, more localized, tensile deformation can occur in the target, e.g. radial fractures [3]. Our goal is to determine how impact-induced deformation varies between different mineralogically homogeneous, non-porous rocks and address their potential influence on the resulting crater.

Methods: Two hypervelocity impact experiments into quartzite and marble were conducted, using a spherical 2.5 mm steel and iron meteorite projectile, respectively, with densities between 7.8 – 8.1 g/cm^3 and an impact velocity of ca. 5.0 km/s. The crater surface topography was measured with a 3D laser scanner. Craters were sawn in half and thin sections of the crater subsurface were made to analyze subsurface deformation. Orientations of the deformation features were mapped to infer the deformation mechanisms.

Results: The crater scans reveal surprisingly similar crater sizes for marble and quartzite craters, despite a large difference in their quasi-static compressive strengths (60 and 230 MPa, respectively [4]). [4] showed that these results are consistent over a large suite of experiments into marble and quartzite. The depth-diameter (d/D) ratio for the marble crater is 0.11, whereas it is 0.14 for the quartzite crater.

Subsurface analysis of the two craters shows that a common feature of both is the development of tensile fractures directly beneath the crater floor due to dilatancy upon pressure release (yellow lines in Fig. 1). Their main characteristic is their subconcentric to subhorizontal orientation relative to the point of impact, which makes them clearly distinguishable from other impact induced fractures. Tensile fractures in both target materials show a large degree of opening (<110µm) at the crater floor, which constantly decreases with depth. However, the maximum depth of tensile failure below the crater floor varies with target material: quartzite 2.2 d_p, marble 1.5 d_p (d_p: projectile diameters, Fig. 1).

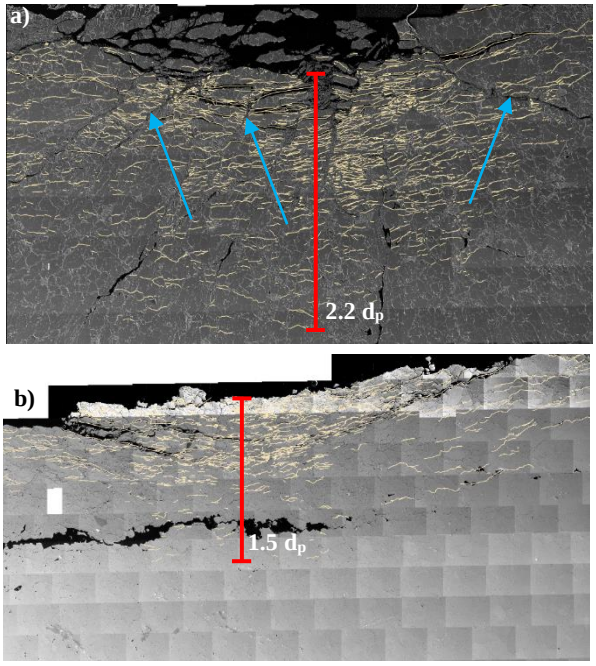

Fig. 1: a) Tensile fractures (yellow lines) beneath the crater floor in a quartzite target into a depth of 2.2 dp (red mark). Localized subradial zones of comminution are marked with blue arrows. b) Tensile fractures (yellow lines) beneath the crater floor in a marble target into a depth of 1.5 dp (red mark).

The quartzite target additionally shows localized deformation along discrete, 25 to 180 µm wide zones (dark blue boundary, Fig. 2a) of subradial orientation relative to the impact point. Target material within these zones is highly comminuted, and these zones are commonly surrounded by areas with larger fractures (light blue hatched area in Fig. 2a). The more distal localized deformation zones closer to the target surface have increasingly flatter and less radial orientations. Furthermore, grain comminution decreases until the

zones show a strong resemblance with step faults. Outside of these fault zones the quartzite target suffered only the formation of narrow radial fractures with an estimated increase in fracture density from the crater floor down to ~1 d_p depth. Radial fractures occur down to a depth of at least 8.5 d_p.

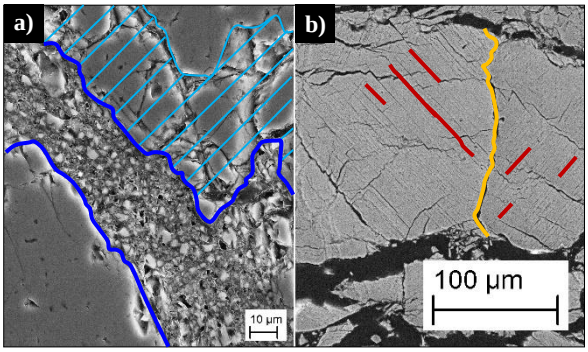

Fig. 2: a) Localized comminution zone in quartzite target, showing intensive grain size reduction (between dark blue boundaries), with a neighboring fracture zone (light blue hatched area). b) Typical intragranular fractures along cleavage planes in calcite (dark red), as well as a cracked grain boundary (orange) in the immediate crater subsurface in a marble target.

In comparison, the marble target experienced intensive and pervasive intra- and intergranular fracturing, but did not develop the localized fracture zones seen in the quartzite target. The intragranular fractures show a stong correlation to the natural cleavage of calcite and a high percentage of the intragranular fractures is crystallographically orientated. In combination with the intergranular and tensile fractures they led to a much stronger overall comminution in the marble subsurface than in the quartzite. A further impact-induced deformation feature is microtwinning along crystallographic planes in calcite minerals and results in minor crystal-plastic behavior of the calcite. Close to the crater floor several sets of twins per grain developed, but with increasing distance to the crater floor their abundance decreases to a depth of ~2 d_p.

The depth of observable deformation features in quartzite extends down to ~ 11.4 d_p, compared to only 3.6 d_p in the marble target. In both targets, the deformation in the most proximal, highly comminuted area underneath the crater floor seems to be controlled by shear deformation. Such a dominance of one deformation mechanism over others cannot be established in the deeper regions of the crater subsurface.

Discussion: The compressive and subsequent tensile stress fields generated in the shock wave are demonstrated by distinct deformation featuers in both target materials.

The strong grain comminution in the localized deformation zones in quartzite indicates compressive failure due to shearing under differential stresses. The apparent absence of deformation in the neighboring areas of the shear zones is probably attributed to the lack of cleavage in quartz. The radial fractures are suggested to form due to hoop stresses in the elastic decay regime [3].

The less localized and more pervasive deformation in the marble target on the other hand can be attributed to the weaker crystal strength of calcite. The excellent rhombohedral cleavage and the possibility of twin formation led to a stronger absorbtion of impact energy by the formation of cleavage fractures and twins. Thus, the shock wave is more effectively dampened than in the quartzite.

Concentric tensile fractures are a common feature of both target materials and are most likely generated by relaxation of volumetric compression upon shock pressure release. These fractures are presumably enhanced by the rarefaction wave. The decrease in the degree of opening of the tensile fractures with depth should correlate with the reduction of tensile stresses of the shock and rarefaction wave.

The different styles of deformation and the resulting dampening of the shock wave in marble might explain why both craters have similar volumes despite their large variation in stregnth, as well as why the the marble craters are shallower in depth.

Conclusions: First results of SEM microscopy of impacted quartzite and marble target subsurfaces reveal great differences in impact induced deformation mechanisms between the two non-porous target materials. The origin of these differences seems mostly to be found in the dynamic mechanical properties of the main rock-forming minerals. Further investigations will be performed to validate these preliminary results.

References: [1] Collins (2014), J. Geophys. Res. Planets, 119, 2600–2619. [2] Ai H.-A. and Ahrens T. J. (2004) Meteoritics & Planet. Sci, 39, 233-246. [3] Poelchau M. H. et al. (2015) LPSC Abstract #2447. [4] Polanskey C. A. and Ahrens T. J. (1990) Icarus, 87,140-155.